Robotica (2005) volume 23, pp. 355–364. © 2005 Cambridge University Press
doi:10.1017/S0263574704000979 Printed in the United Kingdom

Misalignment estimation and compensation for robotic assembly with uncertainty

J. Y. Kim*, W. S. Kim** and H. S. Cho†

(Received in Final Form: July 28, 2004)

SUMMARY

The complexity and uncertainty of the cross-sectional shape of the parts to be mated is one of the main reasons that misalignment between them occurs in assembly processes. Misalignment cannot only give rise to assembly failure but also cause damage to the parts or a robot due to large contact force. Therefore, misalignment sensing and compensation is essential for successful assembly operation. In this paper, we propose a novel misalignment estimation and compensation method which does not need any advance information on the cross-sectional shapes of the mating parts. This method utilizes a $\varphi - r$ transformation and an M-estimation pattern matching technique with misalignment images of a peg and a hole taken by an omni-directional visual sensing system during assembly. At every sampling instant during assembly action, it furnishes information on the relative position and orientation between the mating parts, and thus helps to estimate and compensate any possible misalignment between them. Also, a series of experiments are performed with a couple of peg-in-hole tasks, and the results are discussed. The experimental results show that the proposed method is effective for misalignment compensation in robotic assembly even though there is no prior information on part geometry and the images are very noisy.

KEYWORDS: Misalignment compensation; Robotic assembly; Cross-sectional shape; M-estimation; Omni-directional sensing system.

1. INTRODUCTION

A flexible assembly system (FAS) for small quantity batch production can handle several and different kinds of parts in each stage due to its flexibility. Robotic assembly is one of the effective means implementing such FAS. One of the difficulties that occur during part mating of robot-based assembly is a misalignment problem, which is defined as the relative position and orientation between mating parts. Misalignment can not only give rise to assembly failure but also cause damage to the parts or a robot due to large contact force. Therefore, misalignment sensing and compensation is essential for successful assembly operation.[1]

In order to find misalignment, information on the relative position and orientation between the parts to be mated is necessary, and it can be obtained from the relative cross-sectional geometry between the parts. Therefore, there is a need for a robotic assembly system to have the capabilities to estimate misalignment during assembly and to overcome any uncertainties arising from shape complexity, although the cross-sectional shapes of the parts are not known in advance.

Misalignment can be detected by a number of techniques using a force/torque sensor, a proximity sensor or a visual sensor.[2–5] Among them, a visual sensing technique is often incorporated into an assembly system since it can detect the shape of a part at a distance, as well as a large misalignment. However, a visual sensing system usually obtains only local information due to self-occlusion problem, i.e. some regions are occluded by the mating part itself in the viewing direction. For this reason, it is generally not easy to estimate the misalignment between mating parts with complicated cross-sectional shapes.

In order to overcome the self-occlusion and the difficulties due to geometrical complexity, Miura[6] introduced a camera relocation method. However, this is very time-consuming because it needs image processing of several images and relocating a camera. To solve this problem, the authors have developed an omni-directional sensing system using double conic mirrors.[7,8] This system can overcome self-occlusion, and detect immediately the misalignment between mating parts. Besides, it can overcome the difficulties caused by shape complexity in detecting the misalignment. In case of a peg-in-hole assembly task, however, it is not easy to discern a peg and a hole separately in a misalignment image taken during assembly operation without any advance information on their relative motion and geometry.

Many researches have been done to develop a method on how to discern the mating parts from each other, i.e. a peg and a hole in a misalignment image. One of them utilizes a CAD-based model to obtain geometrical information.[9,10] However, this requires an additional model to handle uncertainty even though it is not easy to construct the model coping with unexpected environmental change. And, there is a method based on image processing, such as chain coding or edge following.[11] In addition, there are many researches using *AI* techniques, such as inductive learning,[12] fuzzy[13] or neural network[14] which deals with a geometrical model, including

* Corresponding author: Department of Mechatronics Engineering, Tongmyong University of Information Technology 535, Yongdang-dong, Nam-gu, Busan 608-711 (South Korea) E-mail: kjy97@tit.ac.kr
** Bioptro Co. LTD., Technopark, #D-801 151, Yatap-dong, Bundang-gu, Sungnam City, Kyungki-do 463-070 (South Korea) E-mail: tobero@dreamwiz.com
† Department of Mechanical Engineering, Korea Advanced Institute of Science and Technology 373-1, Kusong-dong, Yusong-gu, Daejon (South Korea) E-mail: hscho@lca.kaist.ac.kr

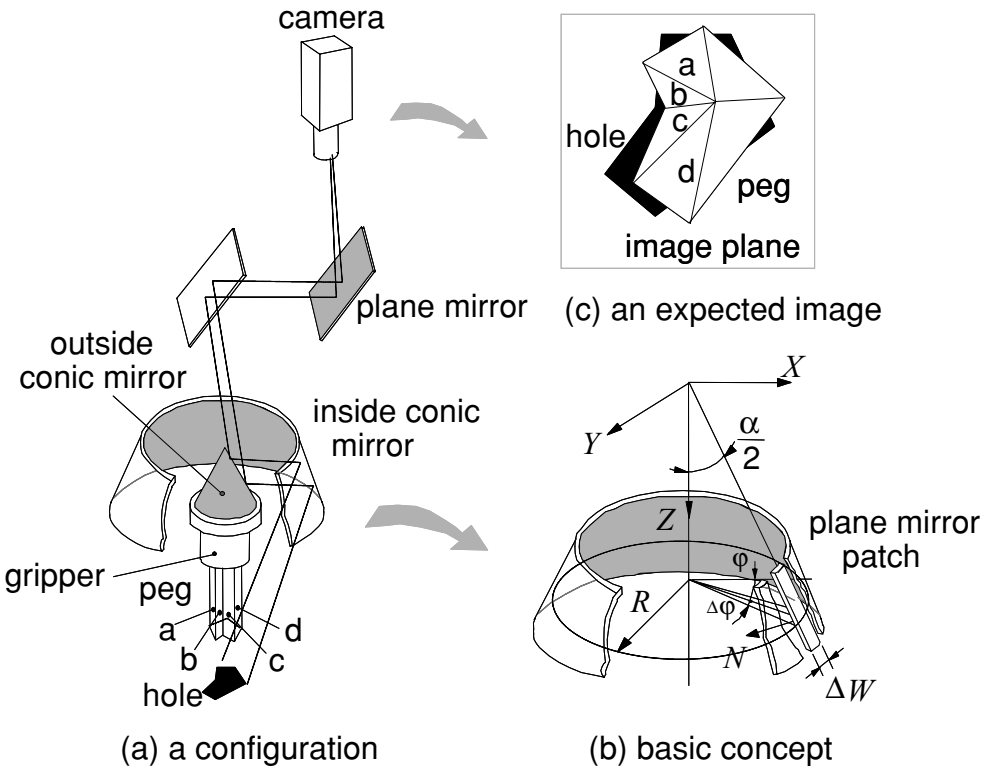

Fig. 1. Schematic diagram of the omni-directional sensing system.

uncertainties. These methods are considerably capable of adapting to the changeable environment for themselves, but they need a great number of learning data or experience-based rules. Also, they need a time-consuming learning procedure to construct a new assembly strategy in accordance with a change of assembly conditions, since the data and rules depend largely on the change.

In this paper, we propose a novel method to estimate and correct the misalignment between the mating parts by discerning a peg and a hole from each other even though their relative geometrical information is not given in advance. This method utilizes an omni-directional sensing system that can obtain the 2π misalignment image between the mating parts. From the edge information, the geometric relations, such as the relative position and orientation between the mating parts are obtained. A pattern matching technique using a $\varphi - r$ transformation and an M-estimation is used to differentiate a peg and a hole from each other in one image of a peg and a hole, and at the same time to correct misalignment between them. And a series of experiments are performed with the parts having circular and rectangular-shaped cross-sections in order to investigate the performance of the proposed method.

The paper is organized as follows: section 2 proposes an effective method to recognize a peg and a hole separately in a misalignment image taken by an omni-directional sensing system without prior information on part geometry. It describes the results obtained from a series of experiments to show the effectiveness of the proposed method. section 3 describes a robust pattern matching method to correct the misalignment between the mating parts. Finally, section 4 draws some conclusions.

2. RECOGNITION OF A PEG AND A HOLE

2.1. Misalignment detection by an omni-directional sensing system

Let us assume that an omni-directional sensing system is used in order to obtain the misalignment image formed by mating parts, because it has a capability of detecting the 2π image of the boundary interface between misaligned parts without self-occlusion, as described in section 1. Fig. 1(a) illustrates a basic configuration of the sensing system. The detailed explanation about the system such as the mapping principle and features can be referred to in reference [7]. The system consists of four components: an inside-conic mirror and an outside-conic mirror, a pair of plane mirrors, a camera, and a gripper. The goal of the sensing system is to obtain a 2π coaxial image without self-occlusion. The inside-conic mirror is a configuration obtained by the 360° rotation of the finite patch of a plane mirror with respect to the vertex axis, as shown in Fig. 1(b). With this configuration, the inside conic mirror is capable of reflecting the 2π figure of an object encompassed by the mirror itself without self-occlusion. In this way, the inside-conic mirror is used to obtain the 2π cross-sectional geometry of the mating part without self-occlusion.

However, additional optical components are required to detect 2π shape by using a camera on off-axis, as shown in Fig. 1(a). First, an outside-conic mirror, placed co-axially at the center of the inside-conic mirror is used to collect the 2π image captured in the inside-conic mirror surface. The collected 2π image is projected onto the image plane of the camera, using two plane mirrors: one is placed above the outside-conic mirror and the other is placed below

https://doi.org/10.1017/S0263574704000979 Published online by Cambridge University Press

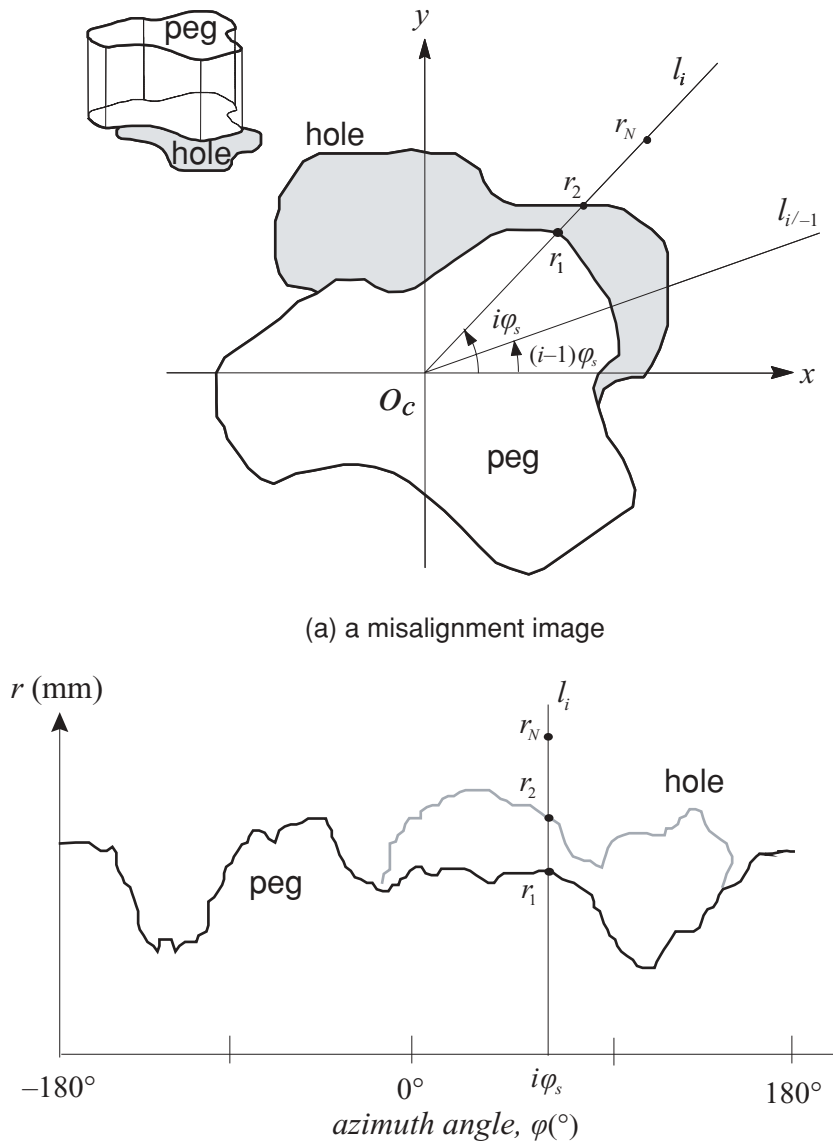

Fig. 2. Conceptual illustration of a $\varphi - r$ algorithm.

the camera, as shown in Fig. 1(a). According to this principle, this system is eventually capable of obtaining not only a 2π coaxial image of the combined shape formed between a peg and a hole without self-occlusion, but also omni-directional side-views such, as figures denoted as a, b, c and d, as shown in Fig. 1(c).

2.2. Problem statements

Figure 2(a) shows a conceptual diagram of the misalignment image detected by the omni-directional sensing system. This 2π coaxial shape is generally characterized according to the double conic projection[8] when a peg with arbitrary shape is captured by the omni-directional sensing system, as shown in the top left of Fig. 2(a). To make the problem simple, let us assume that a peg and a hole are rigid and the cross-sectional shapes are previously not known. Then, the obtained 2π coaxial image reveals several helpful cues to discern a peg and a hole, as stated below.

(a) There is no shape deformation for a peg and a hole during the mating period, and their cross-sectional shapes are identical.
(b) A peg exists above a hole during the mating period, and thus the hole shape is always occluded by a peg shape. In this case, the same part of the boundary edge of the hole is cut by that of the peg.
(c) Cross-sectional shapes of a peg and a hole in a misalignment image remain unchanged, and they have a relation of an Euclidean transformation.

2.3. Feature extraction by $\varphi - r$ transformation

In order to correct misalignment, it is necessary to discern a peg and a hole from each other. And, based on this

https://doi.org/10.1017/S0263574704000979 Published online by Cambridge University Press

information, the size and the direction of misalignment in the course of assembly are identified. Finally, misalignment is corrected for successful assembly. In this paper, we introduce an efficient feature based method to extract the features for discerning a peg and hole. First, let us set up an xy-coordinate system centered at an image center O_c in the misalignment image, as shown in Fig. 2(a). Then, the azimuth angle φ is defined as a counterclockwise angle with respect to the x-axis in the coordinates. Let us call the angle φ_s the sampling angle, with which the number of the sample is given when the 2π angle is divided at an interval of φ_s. We draw radial lines at the interval of φ_s starting from the center O_c outward in a misalignment image plane. Then, a radial line l_i that the azimuth angle φ_i is equal to $i\varphi_s$ among them is defined as follows;

$$y = \tan(\varphi_i) \cdot x, \qquad i = 1, 2, \ldots, \text{int}(2\pi/\varphi_s) \tag{1}$$

where the symbol φ_i represents the azimuth angle of $i\varphi_s$, the subscript i means the i-th line, and the symbol 'int' denotes integer. In addition, the lines encounter point blobs on boundary edges of a peg and hole. All intersection points (φ_i, r_j) are defined as follows;

$$r_j = \sqrt{x_k^2 + y_l^2}, \quad \varphi_i = \tan^{-1}\left(\frac{y_l}{x_k}\right) \tag{2}$$

where the radial distance r_j is defined as the distance from the image center O_c to an intersection point (φ_i, r_j) and (x_k, y_l) is the position of a point blob joined to form the radial line l_i.

Computing the radial distances and transforming them into the $\varphi - r$ space by using the relation (2), the $\varphi - r$ graph is then obtained, as shown in Fig. 2(b). Accordingly, representing the radial distances of the points intersecting the line l_i in the $\varphi - r$ space as a set $\mathbf{R}^i$, it is given as follows:

$$\mathbf{R}^i = \{r_1^i, r_2^i, \ldots, r_n^i, \ldots, r_N^i\} \tag{3}$$

where N is the maximum number of radial elements in the set, and the superscript i denotes the i-th radial line l_i at the azimuth angle of φ_i. The set $\mathbf{R}^i$ includes the radial distances to noises, as well as the distances to point blobs on the boundary edges of a peg and a hole in the 2π coaxial misalignment image.

The distribution features of the set $\mathbf{R}^i$ are unknown because the shapes of mating parts is not given *a priori*. Therefore, an algorithm clustering the elements in the set $\mathbf{R}^i$ needs to be proposed, with which the elements are classified in a self-organized manner under consideration of their distribution features.[8] For instance, the first clustered class has a high probability to be classified into a peg, the second has the next highest probability to be classified into a hole and noises, and the other classes having low probability are classified into environment and background noises. The segmentation between boundary shapes of a peg and a hole in a noisy image can be executed by using an appropriate algorithm based on these interesting features.

2.4. Recognition experiments

A series of experiments have been performed with respect to typical pegs whose cross-sectional area has circular and rectangular shapes, as shown in Fig. 3(a) and Fig. 4(a). The experiments have been performed with the sampling angle $\varphi_s = 2.5^\circ$ for the cylindrical peg and $\varphi_s = 2^\circ$ for the three-dimensional rectangular peg.

Figure 3(a) shows the 2π coaxial misalignment image for the three-dimensional cylindrical peg and hole detected by the proposed sensing system. As expected, self-occlusion does not occur. Fig. 3(b) shows the edge image after thinning operation with respect to the misalignment image of Fig. 3(a). Fig. 3(c) indicates the $\varphi - r$ graph of the misalignment image of Fig. 3(b), and Fig. 3(d) shows a procedure searching a peg and a hole in the 2π coaxial edge image through the detection of the intersection blobs along the radial lines drawn at an interval of $\varphi_s = 2.5^\circ$. Fig. 3(e) and Fig. 3(f) show the recognition results of the peg and the hole, in which case the information about shapes and location of the peg and the hole are previously not given.

The results show that, although the thinned image contains various noises, the peg and the hole are recognized easily by using the proposed algorithm. The blobs of the recognized hole becomes rarer than those of the peg because the location far from the center has lower sampling resolution than that of a closer location when the boundary edges are detected by the radial line at an interval of φ_s. The result also shows that the recognized hole includes much more noises than the peg. This is due to the fact that the secondly detected noises are considered as a part of the hole as described in section 2.3, although the hole boundary edge does not exist at the right-hand side of the image, as shown in Fig. 3(b).

Similarly, Fig. 4 shows a procedure recognizing a rectangular peg and a hole. The peg and the hole are detected in a way similar to the case of the circular peg and the hole. The results show that the rectangular peg and the hole are segmented well in a thinned image containing noises. Also, the detected top edge found in Fig. 4(b) is neglected through the correction procedure. The vertical edge noises are completely eliminated according to the procedure described in section 2.4.

In summary, the experimental results show that, although the shapes of a peg and a hole are not given beforehand, they are segmented from the misalignment image through the $\varphi - r$ algorithm. It is shown that they are identified simply by using a few cues such as the distance and the occurrence order in the $\varphi - r$ space, although the edge images contain a lot of noises. In addition, if the cut-off level of noises is increased, it is natural that much more noise be removed. On the other hand, the shapes of the peg and the hole may not be reconstructed correctly. In other words, there is a trade-off between the noise cut-off level and accuracy of reconstruction of real shapes.

Since there is also a similar relationship between sampling angle and searching time, it is necessary to select the sampling angle under consideration of minimum achievable value of the sampling resolution φ_r. In these experiments, it is found that the sampling angle in the range of $1^\circ \sim 2.5^\circ$ and the noise cut-off level of 5 pixels give stable results.

https://doi.org/10.1017/S0263574704000979 Published online by Cambridge University Press

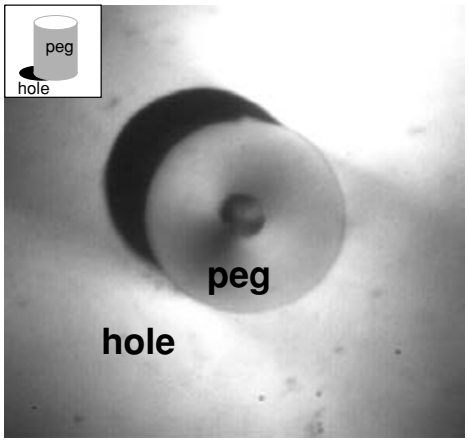

(a) initial misalignment image

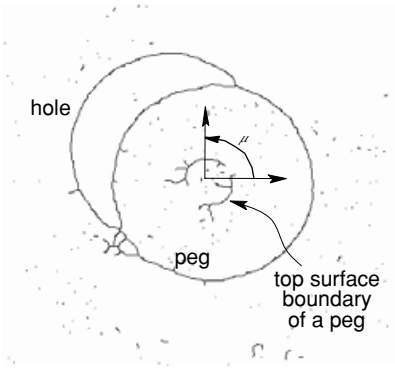

(b) edge image

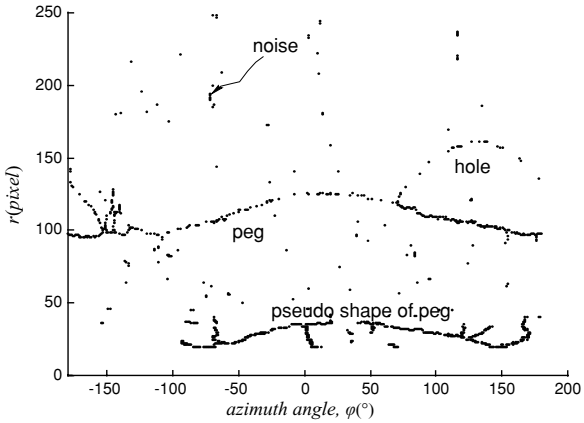

(c) $\varphi - r$ transformation

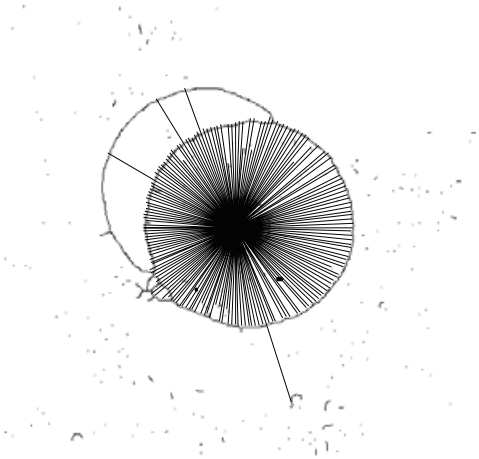

(d) peg searching procedure

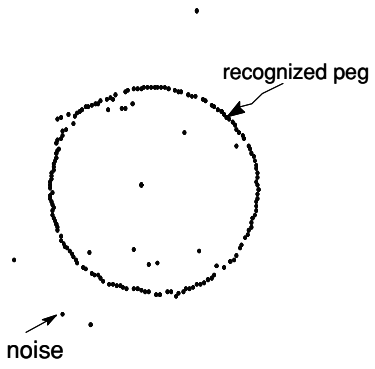

(e) identified peg

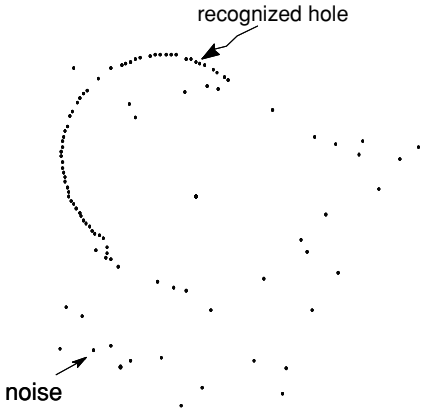

(f) identified hole

Fig. 3. Recognition of a circular peg and a hole.

3. MISALIGNMENT CORRECTION BY ROBUST MATCHING

3.1. Misalignment corrective motion using an M-estimator

According to the precondition (a) described in section 2.2, it is assumed that the shape of a peg and that of a hole appearing in a misalignment image are identical to each other. In order to compensate for identified misalignment under the condition, the peg is moved toward the hole, and then the geometrical shape of the peg is matched to that of the hole. As a method for matching, a transformation between the peg and the hole can be utilized, and it is defined by the

https://doi.org/10.1017/S0263574704000979 Published online by Cambridge University Press

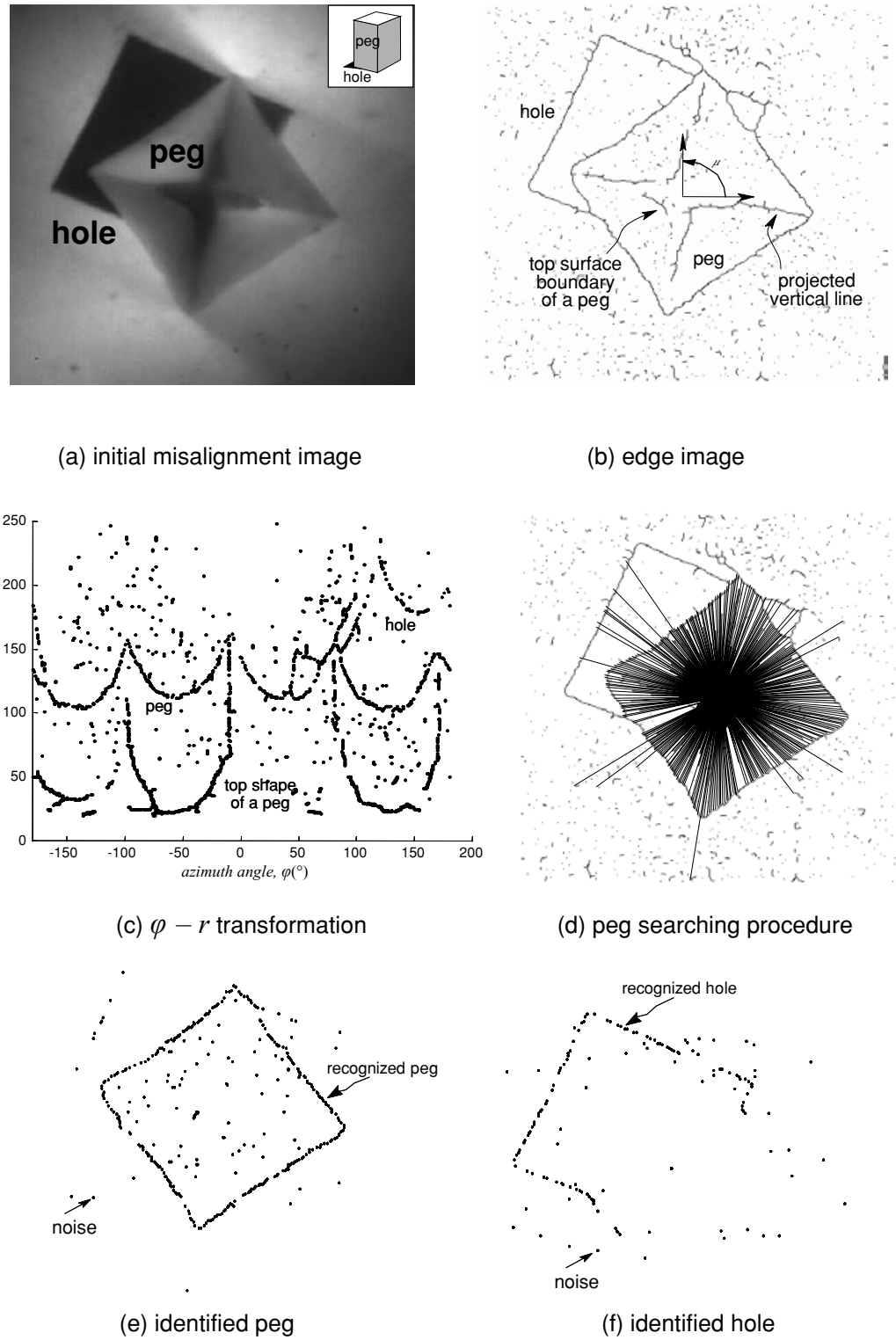

(a) initial misalignment image

(b) edge image

(c) $\varphi - r$ transformation

(d) peg searching procedure

(e) identified peg

(f) identified hole

Fig. 4. Recognition of a rectangular peg and a hole.

motion parameters such as the rotation and the translation between two boundary shapes before and after motion. Let us locate a set of N pairs of corresponding points (p_i, h_i), which are called control points in two shapes of a peg and a hole, $p_i \in P_s$ and $h_i \in H_s$, $i = 1, 2, \ldots, N$, where P_s, H_s is a set of the points which belong to the edge of the peg and the hole respectively. Then, the matching problem is to find the transformation $\mathbf{T}$ that minimizes an error function defined as follows;[15]

$$e = \sum_{i}^{N} |\mathbf{T} \cdot p_i - h_i|^2. \tag{4}$$

https://doi.org/10.1017/S0263574704000979 Published online by Cambridge University Press

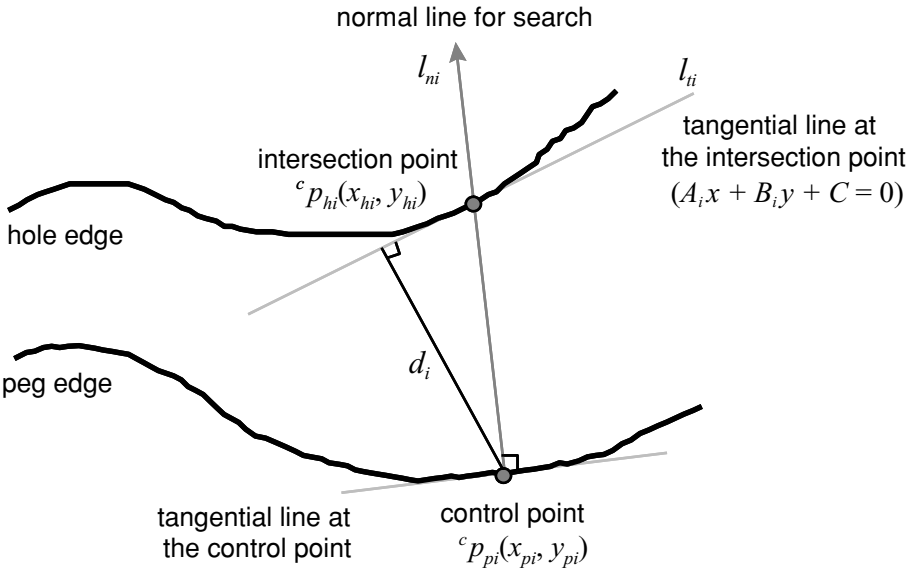

Fig. 5. The distance between two curves to be matched.

However, it is not easy to obtain the transformation by using Eq. (4) for arbitrary curves. As an alternative, minimizing a distance function given in Eq. (5), which is defined by the distances between the points that belong to the edge of the peg and the hole, can be used.

$$e = \sum_{i}^{N} \|\mathbf{T} \cdot p_i - h_i\|^2 \tag{5}$$

Here, $\|\cdot\|$ represents the norm of a matrix. As the peg moves toward the hole, a transformation $\mathbf{T}$ needs to be re-computed repeatedly to obtain more accurate and new transformation. Starting from an initial transformation $\mathbf{T}^0$, it can be represented by an iterative form as follows;

$$e^k = \sum_{i}^{N} \left\|\mathbf{T}^k \cdot p_i^k - h_i\right\|^2 \tag{6}$$

where superscript k denotes an iteration number. In addition, the sensing system obtains a 2π coaxial misalignment image, which remain unchanged, and so the transformation can be considered as an Euclidean transformation, as assumed in the precondition (c) of section 2.2. Hence, it is given as follows;

$$\mathbf{T} = \begin{bmatrix} a & b & c \\ -b & a & d \\ 0 & 0 & 1 \end{bmatrix} \tag{7}$$

where a and b represent the orientation components of the misalignment between a peg and a hole, and c and d represent the position components of the misalignment.

Let us assume that there are two boundary shapes of a peg and a hole detected by an image sensing system, as shown in Fig. 5. Then, ${}^c p_{pi}$ represents a pixel point $(x_{pi}, y_{pi}, 1)^t$ on the boundary edge of a peg in an image, where t denotes the transpose of a vector. The normal distance d_i between a pixel point ${}^c p_{pi} = (x_{pi}, y_{pi}, 1)^t$ and a tangential line l_{ti} is given by

$$d_i = \frac{A_i x_{pi} + B_i y_{pi} + C_i}{\sqrt{A_i^2 + B_i^2}} \tag{8}$$

where the tangential line l_{ti} is defined as $A_i x + B_i y + C_i = 0$. The line l_{ti} is the tangential line at a point ${}^c p_{hi} = (x_{hi}, y_{hi}, 1)^t$ which is the intersection point of the hole boundary and the normal line l_{ni} at a point ${}^c p_{pi} = (x_{pi}, y_{pi}, 1)^t$. Then, based on Eq. (8), the newly modified error function of Eq. (6) is defined as follows;

$$e^k = \sum_i \left(d_i^k\right)^2 = \sum_i \frac{1}{\left(A_i^2 + B_i^2\right)} \left(A_i \left(a x_i^{k-1} + b y_i^{k-1} + c\right) + B_i \left(-b x_i^{k-1} + a y_i^{k-1} + d\right) + C_i\right)^2 \tag{9}$$

where a, b, c, d are the elements of a transformation matrix $\mathbf{T}$, and x_i^{k-1}, y_i^{k-1} denote a point on the peg boundary at (k-1)-th iteration.

However, this function has the same weight factors for all related points regardless of their distance values, and so it can not reduce the effect of the noises which the recognized image of a peg and a hole might contain. In other words, a more robust method is necessary to estimate more accurate motion parameters. This study utilizes an M-estimator which is robust to noisy images.[16,17] The error function of Eq. (9) is then modified by the M-estimation as follows;

$$e^k = \sum_i w\left(d_i^{k-1}\right) \cdot \left(d_i^k\right)^2 \tag{10}$$

https://doi.org/10.1017/S0263574704000979 Published online by Cambridge University Press

where w denotes a weight factor which is defined by

$$w\left(d_i^{k-1}\right) = \begin{cases} 1 & \text{for} \quad d_i \le \sigma \\ \sigma \Big/ \left|d_i^{k-1}\right| & \text{for} \quad \sigma < d_i < 3\sigma \\ 0 & \text{for} \quad d_i > 3\sigma \end{cases} \tag{11}$$

where σ is a constant value such as standard deviation. In other words, the robotic motion parameters for misalignment correction can be obtained by minimizing the error function of Eq. (10) by least square method. Explaining in detail, the least square solutions can be obtained from that the partial derivatives of the error function with respect to the motion parameters are equivalent to zeros. Differentiating the error function with respect to the motion parameters $\mathbf{p}_m = (a, b, c, d)^t$, then $\frac{\partial e^k}{\partial a} = 0$, $\frac{\partial e^k}{\partial b} = 0$, $\frac{\partial e^k}{\partial c} = 0$, $\frac{\partial e^k}{\partial d} = 0$. Solving these equations, the motion parameter vector $\mathbf{p}_m$ is given by

$$\mathbf{p}_m = \mathbf{D}_l^{-1}\mathbf{D}_r \tag{12}$$

where

$$\mathbf{D}_l = \begin{bmatrix} \sum_i w\left(d_i^{k-1}\right)(A_i x_i + B_i y_i)^2 & \sum_i w\left(d_i^{k-1}\right)(A_i y_i - B_i x_i)(A_i x_i + B_i y_i) & \sum_i w\left(d_i^{k-1}\right)A_i(A_i x_i + B_i y_i) & \sum_i w\left(d_i^{k-1}\right)B_i(A_i x_i + B_i y_i) \\ \sum_i w\left(d_i^{k-1}\right)(A_i x_i + B_i y_i)(A_i y_i - B_i x_i) & \sum_i w\left(d_i^{k-1}\right)(A_i y_i - B_i x_i)^2 & \sum_i w\left(d_i^{k-1}\right)A_i(A_i y_i - B_i x_i) & \sum_i w\left(d_i^{k-1}\right)B_i(A_i y_i - B_i x_i) \\ \sum_i w\left(d_i^{k-1}\right)A_i(A_i x_i + B_i y_i) & \sum_i w\left(d_i^{k-1}\right)A_i(A_i y_i - B_i x_i) & \sum_i w\left(d_i^{k-1}\right)A_i^2 & \sum_i w\left(d_i^{k-1}\right)A_i B_i \\ \sum_i w\left(d_i^{k-1}\right)B_i(A_i x_i + B_i y_i) & \sum_i w\left(d_i^{k-1}\right)B_i(A_i y_i - B_i x_i) & \sum_i w\left(d_i^{k-1}\right)A_i B_i & \sum_i w\left(d_i^{k-1}\right)B_i^2 \end{bmatrix}$$

$$\mathbf{D}_r = \begin{bmatrix} -\sum_i w\left(d_i^{k-1}\right)C_i(A_i x_i + B_i y_i) \\ -\sum_i w\left(d_i^{k-1}\right)C_i(A_i y_i - B_i x_i) \\ -\sum_i w\left(d_i^{k-1}\right)C_i A_i \\ -\sum_i w\left(d_i^{k-1}\right)C_i B_i \end{bmatrix}.$$

In conclusion, the motion parameters a, b, c, d can be obtained from Eq. (12) by an iterative operation. On the other hand, the robotic corrective motion also can be represented by using another motion parameter vector $\mathbf{p}_{rm} = (t_x, t_y, \alpha)^t$ as follows:

$$\mathbf{p}_{rm} = \begin{bmatrix} t_x \\ t_y \\ \alpha \end{bmatrix} = \begin{bmatrix} c \\ d \\ \tan^{-1}(b/a) \end{bmatrix} \tag{13}$$

where t_x and t_y denote the translation in x and y direction, and α denotes the orientation angle of the corrective motion.

3.2. Misalignment correction experiments

In order to investigate the effectiveness of the algorithm proposed in section 3.1, a series of experiments were performed under a couple of conditions of part mating. As shown in Fig. 6, misalignment correction experiments were performed by using the pegs and the holes with circular and rectangular cross-sectional shapes, respectively. Fig. 6(a) shows the edge images in the initial position. First, the edge images of a peg and a hole are extracted from the original images such as Fig. 3(a) or Fig. 4(a), which are taken by the omni-directional sensing system. Next, the peg and the hole are recognized separately from the misalignment edge images by using the $\varphi - r$ transformation, which is described in section 2.3.

In these experiments, the boundary edges were sampled at an interval of 4° for the circular cross-sectional shaped peg and hole, and 2° for the rectangular cross-sectional shaped peg and hole. These sampling angles are much larger than the resolution $\varphi_r = 0.24°$ of the implemented sensing system. In the initial position, the misalignment ratio between the circular peg and its corresponding hole is about 60%, and the misalignment ration in the case of the rectangular peg and hole is about 80%. The misalignment ratio is defined as the ratio of the area of the visible part of a hole to the cross-sectional area of a peg.

Fig. 6(b) and Fig. 6(c) show the states after 5 and 10 corrective motion using the proposed corrective matching algorithm. Each time an iteration is executed, the corrective motion parameters of Eq. (13) are computed by the method described in section 3.1. As a result of the robotic corrective motion by the parameters, the peg in the misaligned position is moved gradually to the hole position. In the end, the assembly operation is completed successfully through complex matching. Also, these experimental results show that the proposed algorithm works effectively in noisy images too. Comparing with the two cases of a circular peg and a rectangular peg in these experiments, the rectangular peg needs more iterations to correct the misalignment due to the complexity of the shape. The results indicate that, as the part shape becomes more complicated, the matching process takes longer time and the misalignment correction need more iterations.

On the other hand, there is another factor which has an influence on the misalignment correction, it is misalignment ration. Fig. 7 shows the convergence rate of iterative misalignment correction according to the misalignment ratios of 80%, 70% and 60% in a circular-shaped peg-in-hole task. The results show faster convergence rate as the misalignment ratio is small. Also, a small misalignment ratio results in a short matching time, and so we can select a small sampling angle. However, the cases with small misalignment ratios are more sensitive to noises because the number of data points for matching is small.

From these experimental results, it is concluded that the proposed misalignment corrective method, using the $\varphi - r$ transformation and the M-estimator, is effective in robotic assembly although any information on the part geometry is not given in advance.

https://doi.org/10.1017/S0263574704000979 Published online by Cambridge University Press

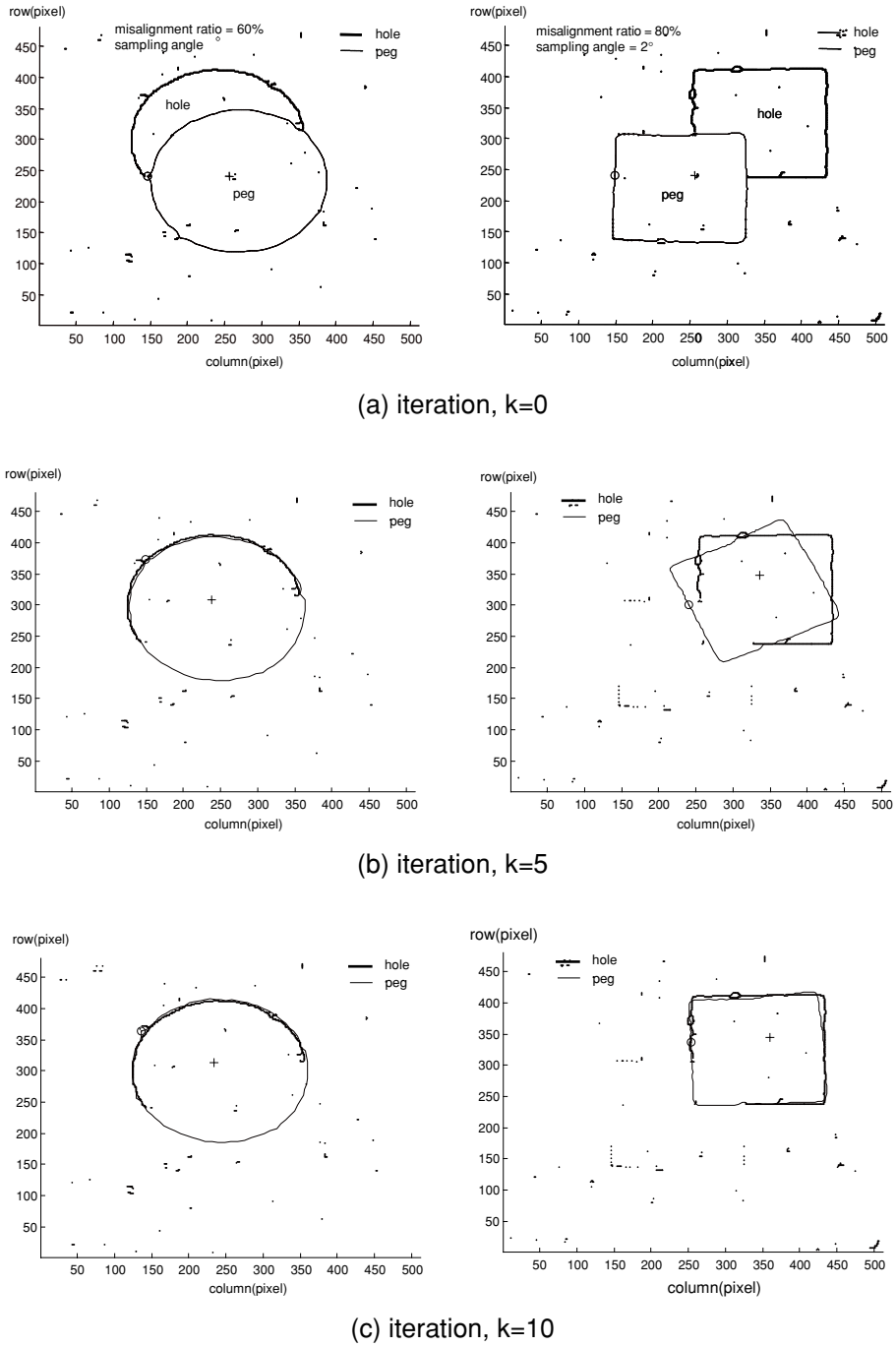

Fig. 6. Correction of misalignment between a peg and a hole.

4. CONCLUSIONS

In this paper, we have proposed a novel method to estimate and correct the misalignment between the mating parts by discerning a peg and a hole from each other in a misalignment image without any advance information on part geometry in robotic assembly. This method utilized an omni-directional sensing system that can obtain the 2π misalignment image between the mating parts. A feature extraction algorithm using a $\varphi - r$ transformation method has been developed to recognize a peg and a hole separately in an image. And, a misalignment corrective algorithm using an M-estimator has been developed on the basis of the misalignment estimation algorithm between the recognized peg and hole. To confirm the effectiveness of the proposed method, a series of experiments have been performed with a couple of part shapes and assembly conditions.

The experimental results show that the proposed method can recognize a peg and a hole effectively by using only a few features such as the distance and the order of occurrence defined in the $\varphi - r$ space, even though the edge images contain a lot of noise. And the misalignment between the mating parts was corrected successfully by using a pattern matching technique in spite of a lot of noise. Therefore, it is concluded that the proposed misalignment corrective

https://doi.org/10.1017/S0263574704000979 Published online by Cambridge University Press

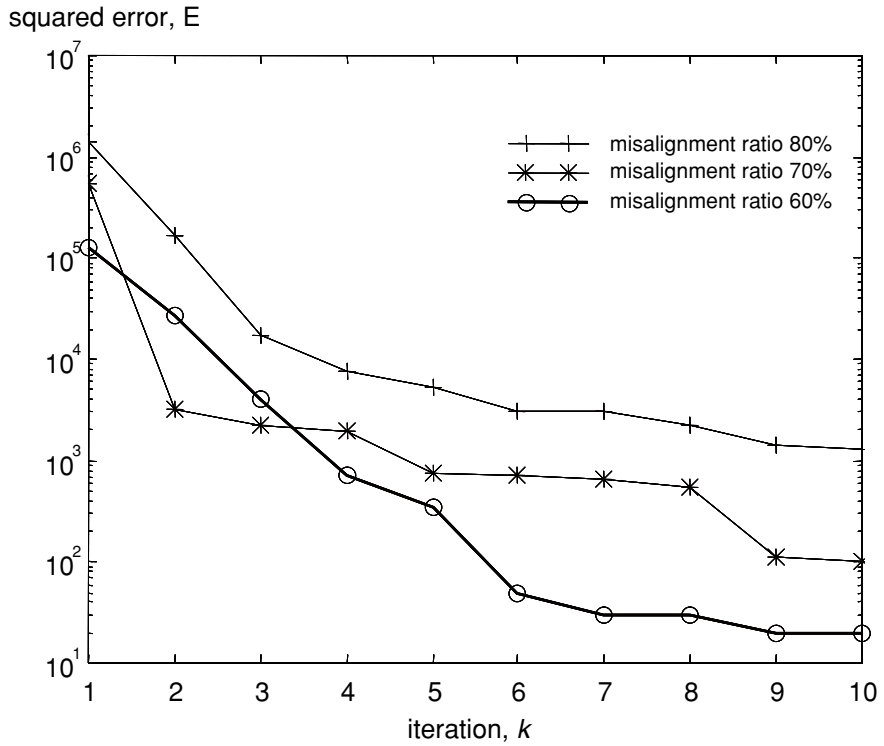

Fig. 7. Convergence rate according to the misalignment ratio.

method using the $\varphi - r$ transformation and the M-estimator is effective in robotic assembly and adapts flexibly to unexpected changes of assembly conditions.

References

1. C. S. G. Lee, R. C. Gonzalez and K. S. Fu, *Tutorial on Robotics* (IEEE Computer Society Press, 1986) pp. 447–565.
2. H. S. Cho, H. J. Warnecke and D. G. Gwon, "Robotic assembly: a synthesizing overview," *Robotica* **5**, Part 2, 153–165 (1987).
3. Y. Zhou, B. J. Nelson and B. Vikranditya, "Integrating optical force sensing with visual servoing for microassembly," *J. Intelligent and Robotic System* **28**, 259–276 (2000).
4. J. Y. Kim, H. S. Cho and S. Kim, "A visual sensing system for measuring parts deformation and misalignments in flexible parts assembly," *Optics and Lasers Engineering* **15**, No. 5, 379–401 (1998).
5. J. Y. Kim and H. S. Cho, "A neural net-based assembly algorithm for flexible parts assembly," *J. Intelligent and Robotic Systems* **29**, No. 2, 133–160 (2000).
6. J. Miura and K. Ikeuchi, "Generating visual sensing strategies in assembly task," *IEEE Int. Conf. on Robotics and Automation* (1995) pp. 1912–1918.
7. W. S. Kim and H. S. Cho, "A new omni-directional image sensing system for assembling parts with arbitrary cross-sectional shapes," *IEEE/ASME Trans. on Mechatronics* **3**, No. 4, 275–292 (1998).
8. W. S. Kim, H. S. Cho and S. Kim, "Distortion analysis in an omni-directional image sensing system for assembly," *IEEE Symp. on Assembly and Task Planning* (1997) pp. 257–262.
9. C. S. G. Lee and E. S. H. Hou, "Automatic generation and synthesis of C-frames for mechanical parts in an insertion task", *IEEE J. of Robotics and Automation* **4**, No. 3, 287–293 (1988).
10. T. Lozano-Perez, M. T. Mason and R. H. Taylor, "Automatic synthesis of fine-motion strategies for robots," *Int. J. of Robotics Research* **3**, No. 1, 3–24 (1984).
11. D. H. Ballard and C. M. Brown, *Computer Vision* (Prentice Hall, Inc. 1982).
12. B. Dufay and J. Latombe, "An approach to automatic robot programming based on inductive learning," *Int. J. of Robotics Research* **3**, No. 4, 3–20 (1984).
13. Y. K. Park and H. S. Cho, "A fuzzy rule-based assembly algorithm for precise parts mating," *Mechatronics* **3**, No. 4, 433–450 (1993).
14. H. Asada, "Teaching and learning of compliance using neural nets: Representation and generation of nonlinear compliance," *IEEE Int. Conf. on Robotics and Automation* (1990) pp. 1237–1244.
15. R. M. Haralick and L. G. Sappiro, *Computer and Robot Vision* (Addison-Wesley Co., Vol. II, 1992) pp. 167–178.
16. Z. Zhang, "Parameter estimation techniques: a Tutorial with application to conic fitting," *INRIA Technical Report*, No. 2676 (1995).
17. P. J. Hubber, *Robust Statistics* (John Wiley & Sons, 1981).

https://doi.org/10.1017/S0263574704000979 Published online by Cambridge University Press